Competition between electron and hole stimulated Raman passage

Petr Král,[1,2] Jaromír Fiurášek,[1] and Moshe Shapiro[1,2]
[1]*Department of Chemical Physics, Weizmann Institute of Science, 76100 Rehovot, Israel*
[2] *ITAMP, Harvard-Smithsonian Center for Astrophysics, Cambridge, Massachusetts 02138*
(Received 15 February 2001; published 9 July 2001)

We demonstrate an *electron-hole symmetry* in the method of stimulated Raman adiabatic passage (STIRAP), and point out the existence of separate electron and hole regimes in atoms and molecules. In particular, we study hole STIRAP's in the triplet states of N_2. We show that when electron and hole STIRAP's coexist, the competition between them leads to a powerful method of controlling bifurcating processes in molecular systems.

DOI: 10.1103/PhysRevA.64.023414 PACS number(s): 42.50.Md, 33.80.Be, 42.50.Hz, 78.40.Ri

I. INTRODUCTION

In a stimulated Raman adiabatic passage (STIRAP) [1], quantum systems can be transferred from an initial state $|1\rangle$ through an intermediate state $|2\rangle$ to a final state $|3\rangle$, by a sequence of two one-photon transitions. A STIRAP has a nearly 100% efficiency due to the presence of *dark states*, which adiabatically lead the system to the chosen final states.

The method was experimentally verified in the 1980s [2], and is currently being applied in a large number of diverse fields [3], like the laser control of chemical reactions [4], atom optics and manipulation [5], and molecular photoassociation of ultracold atoms [6]. It may even have some bearing on recent photoassociation experiments in Bose-Einstein condensates [7]. Dark states are also broadly used in atomic cooling by cw fields [8] and in electro-magnetically induced transparency [9], recently studied for hole states [10].

In this work, we point out that a STIRAP can have two forms, *electron* and *hole*, depending on whether an orbital active in the intermediate state is empty or populated. Since, in these two regimes the sequence of pulses is inverted, the method has a full *electron-hole symmetry*. We explore quantum interference resulting from competition between the electron and hole STIRAP's.

II. ELECTRON-HOLE SYMMETRY IN STIRAP'S

In Fig. 1(a), we present a scheme of the electron and hole STIRAP's in a three-orbital system. The empty (full) orbitals are drawn with empty (full) circles. On the left, we show an electron STIRAP: an electron, occupying orbital $|1\rangle$, passes through the empty orbital $|2\rangle$, ending up in an unoccupied orbital $|3\rangle$. This process is executed in a ''counterintuitive'' pulse ordering, in which a laser pulse *A* is turned on first. On the right-hand side, we depict a hole STIRAP, where a hole residing in orbital $|3\rangle$ passes through an occupied orbital $|2\rangle$ to an occupied orbital $|1\rangle$. In this case, a pulse *B* is turned on first.

In this three-orbital system with one (two) electrons, the Hilbert space is spanned by the total electronic states

$$|1_e\rangle=|100\rangle,\quad |2_e\rangle=|010\rangle,\quad |3_e\rangle=|001\rangle,$$
$$|1_h\rangle=|011\rangle,\quad |2_h\rangle=|101\rangle,\quad |3_h\rangle=|110\rangle, \tag{1}$$

where the $|ijk\rangle$ $(i,j,k=0,1)$ notation displays the population of orbitals $|1\rangle$, $|2\rangle$, and $|3\rangle$, respectively. The state $|j_e\rangle$ ($|j_h\rangle$) can be viewed as single electrons (holes); hence the subscript e (h). In Fig. 1(b), we show that the two regimes are realized by transitions $|1_e\rangle\rightarrow|2_e\rangle\rightarrow|3_e\rangle$ and $|3_h\rangle\rightarrow|2_h\rangle\rightarrow|1_h\rangle$, respectively.

We can examine a hole STIRAP using the Hamiltonian

$$H=\sum_{j=1}^{3}\hbar\omega_j|j_h\rangle\langle j_h|+(\hbar\Omega_{12}(t)e^{-i\omega_{12}t}|1_h\rangle\langle 2_h|+\text{H.c.})$$
$$+(\hbar\Omega_{32}(t)e^{-i\omega_{32}t}|3_h\rangle\langle 2_h|+\text{H.c.}). \tag{2}$$

Here $\hbar\omega_j$ are energies of the composite states $|j_h\rangle$, $\Omega_{ij}(t)=\Omega_{ji}^{*}(t)=\mu_{ij}\mathcal{E}_{ij}(t)/\hbar$ are time-dependent Rabi frequencies. $\mathcal{E}_{ij}(t)$ and ω_{ij} denote amplitudes and frequencies of the laser fields, which couple the states $|1_h\rangle$, $|3_h\rangle$, and $|2_h\rangle$ by the dipole elements μ_{12} and μ_{32}.

In the presence of the laser fields, we can write the wave function of the system as

$$|\psi(t)\rangle=C_1(t)e^{-i(\omega_2+\omega_3-\Delta_1)t}\ |1_h\rangle+C_2(t)e^{-i(\omega_1+\omega_3)t}\ |2_h\rangle$$
$$+C_3(t)e^{-i(\omega_1+\omega_2-\Delta_3)t}\ |3_h\rangle, \tag{3}$$

where the detunings are

$$\Delta_j=\omega_{j2}-\omega_j+\omega_2,\quad j=1,3. \tag{4}$$

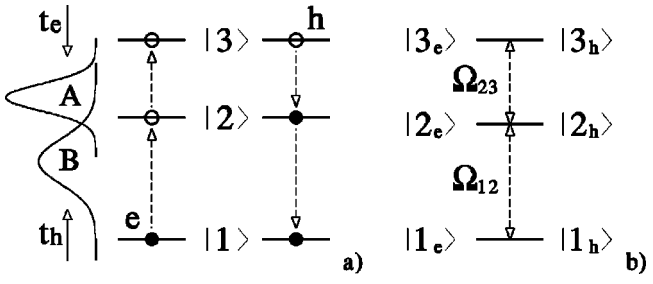

FIG. 1. (a) Scheme of the electron and hole STIRAP's with transitions shown between the orbitals $|1\rangle\rightarrow|2\rangle\rightarrow|3\rangle$ and $|3\rangle\rightarrow|2\rangle\rightarrow|1\rangle$, respectively. (b) Electron and hole STIRAP as viewed in the total electronic states. The field with the Rabi frequency Ω_{23} (Ω_{12}) is turned on first in the electron (hole) STIRAP.

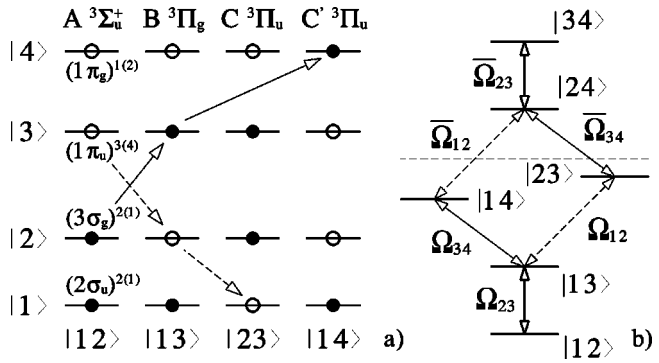

FIG. 2. (a) Electron (hole) STIRAP in a four-orbital system with two electrons initially in orbitals $|1\rangle$ and $|2\rangle$; the relevant population of orbitals for energy terms in N_2 is also denoted. The electron (hole) STIRAP transitions are shown by solid (dashed) arrows. (b) An equivalent scheme, where each level corresponds to a two-electron state.

We can evaluate the vector of slowly evolving coefficients $\mathbf{C}(t)=(C_1,C_2,C_3)^T$ from the Schrödinger equation

$$\dot{\mathbf{C}}(t)=-i\,\mathbf{H}(t)\,\mathbf{C}(t), \tag{5}$$

where the effective Hamiltonian is

$$\mathbf{H}(t)=\begin{bmatrix}\Delta_1 & \Omega_{12}^*(t) & 0\\ \Omega_{12}(t) & 0 & \Omega_{32}(t)\\ 0 & \Omega_{32}^*(t) & \Delta_3\end{bmatrix}. \tag{6}$$

The discussion is simplest [3] when both laser pulses are tuned to resonance: $\Delta_j=0$.

From the three adiabatic eigenstates of the effective Hamiltonian [Eq. (6)], of particular interest is the dark state with a zero eigenvalue, expressed as

$$\mathbf{C}_D(t)=(\cos\theta(t),\,0,\,\sin\theta(t)e^{i\varphi(t)})^T, \tag{7}$$

where

$$\tan\theta(t)=\left|\frac{\Omega_{12}(t)}{\Omega_{32}(t)}\right|,\quad \varphi(t)=\mathrm{Arg}\,\frac{\Omega_{12}(t)}{\Omega_{32}(t)}+\pi.$$

In the counterintuitive hole STIRAP scheme, shown in Fig. 1, the system follows the dark state $\mathbf{C}_D(t)$. In this state, as the phase $\theta(t)$ goes from $\theta(0)=\pi/2$ to $\theta(\infty)=0$, the hole adiabatically passes from the state $|3_h\rangle$ to the state $|1_h\rangle$. Therefore, the electron and hole formalisms are completely analogous.

III. ELECTRON AND HOLE STIRAP SYSTEMS

From the description in Fig. 1, we can unambiguously decide if a particular atomic or molecular STIRAP has an electron or hole character. The classification is based on whether one or two electrons *jump* between the three involved orbitals [also see Fig. 2(a)]. This holds even if the initial and final electronic states are the same, differing only in their rovibronic assignments, as in molecules like NO, SO_2 [3] and benzene [11]. Practically speaking, a hole STIRAP can be more easily realized in molecules, because in atoms the laser energies are required to bridge over different shells, with energy differences larger than 10 eV, almost comparable with atom ionization energies.

To be specific, we concentrate on a hole STIRAP in the N_2 molecule. The assignment of the ground electronic state $X\ ^1\Sigma_g^+$ is $(1\sigma_g)^2(1\sigma_u)^2(2\sigma_g)^2(2\sigma_u)^2(1\pi_u)^4(3\sigma_g)^2$. The transitions we consider are between the triplet states [12,13] $A\ ^3\Sigma_u^+\rightarrow B\ ^3\Pi_g\rightarrow C\ ^3\Pi_u$, whose valence assignments are $\underline{(1\pi_u)^3}(1\pi_g)^1\rightarrow\underline{(3\sigma_g)^1(1\pi_g)}^1\rightarrow\underline{(2\sigma_u)^1(1\pi_g)}^1$. Here we underline the moving hole [also see Fig. 2(a)] and show only those electronic occupations differing from the singlet state $X\ ^1\Sigma_g^+$. The metastable state $A\ ^3\Sigma_u^+$ decays radiatively, with a lifetime of [14] $\tau_{A\rightarrow X}\approx 1$ s, to the ground state $X\ ^1\Sigma_g^+$. Radiative transitions between the ground vibrational states of the $C\ ^3\Pi_u$, $B\ ^3\Pi_g$, and $A\ ^3\Sigma_u^+$ manifolds have the frequencies [14] $\nu_{CB}\approx 29670\ \mathrm{cm}^{-1}$ and $\nu_{BA}\approx 9557\ \mathrm{cm}^{-1}$. The transition times are $\tau_{CB}\approx 72.5$ ns and $\tau_{BA}\approx 15.2\ \mu$s. Using the expression for the Einstein A coefficient [11], we obtain that the related dipole matrix elements are $\mu_{CB}\approx 4.31\times 10^{-30}$ C m (Coulomb meter) and $\mu_{BA}\approx 1.63\times 10^{-30}$ C m. The transition time τ_{CB} necessitates the use of a pulse whose duration is of the order of a few ns. At these durations, adiabaticity can be maintained by Rabi frequencies of $\Omega_{CB}\approx\Omega_{BA}\approx 10^{10}\ \mathrm{s}^{-1}$, i.e., fields of $E_{CB}\approx 2.3$ kV/cm and $E_{BA}\approx 6.3$ kV/cm.

IV. COUPLED ELECTRON-HOLE STIRAP'S

An interesting situation arises when electron and hole STIRAP's *coexist* and *compete* with each other. This can be realized in a model composed of four orbitals $|i\rangle 1\leq i\leq 4$, of which only two are always populated, shown in Fig. 2(a). An electron (hole) STIRAP transfers an electron (hole) from state $|2\rangle$ ($|3\rangle$) through state $|3\rangle$ ($|2\rangle$) to state $|4\rangle$ ($|1\rangle$), shown by the solid (dashed) arrows. For example, in N_2, we can assign orbitals $|1\rangle$ and $|2\rangle$ to orbitals $2\sigma_u$ and $3\sigma_g$, respectively, while orbitals $|3\rangle$ and $|4\rangle$ correspond to the orbitals $1\pi_u$ and $1\pi_g$, respectively. In the considered STIRAP transitions, orbitals $2\sigma_u$, $3\sigma_g$, and $1\pi_u$ have one or two electrons, and orbital $1\pi_g$ has three or four electrons. Hole states are attributed to the lower occupation number in each respective orbital. In this notation, the two-electron states $|ij\rangle$, $1\leq i<j\leq 4$, correspond to the configurations in N_2 [13]: $A\ ^3\Sigma_u^+=|12\rangle$, $B\ ^3\Pi_g=|13\rangle$, $C\ ^3\Pi_u=|23\rangle$, and $C'\ ^3\Pi_u=|14\rangle$. Thus, in an electron STIRAP, moving an electron between the orbitals $(3\sigma_g)^2\rightarrow(1\pi_u)^4\rightarrow(1\pi_g)^2$ corresponds to transitions $A\ ^3\Sigma_u^+\rightarrow B\ ^3\Pi_g\rightarrow C'\ ^3\Pi_u$.

In Fig. 2(b), electron (hole) STIRAP transitions between the two-electron states $|ij\rangle$ are shown by the left (right) full (broken) arrows. Boldface vertical arrows indicate delayed transitions common to the two STIRAP's. We might expect that additional radiative transitions are possible, shown above the horizontal thin dashed line, to the level $|24\rangle$ e-h symmetric with respect to states $|13\rangle$ and $|34\rangle$ e-h symmetric with state $|12\rangle$. Since, electronic interactions detune the energy terms in different amounts, these transitions could be

achieved by separate excitations ($\bar{\Omega}_{ij}$) of a time ordering as in the lower part of the scheme (Ω_{ij}). The augmented scheme would also work if we substitute states $|24\rangle$ and $|34\rangle$ with electronic states $|13\rangle$ and $|12\rangle$, with nonzero rovibronic occupation [14].

A. Description of the electron-hole STIRAP

We now come to the main point of our study, namely, the *competition* between the coexisting electron and hole STIRAP's. We describe this augmented six-level scheme by a wave function expanded as $|\Psi\rangle = \Sigma_{i<j\leqslant 6} C_{ij}(t)\, e^{-i(\omega_i+\omega_j)t}|ij\rangle$, where resonant conditions are considered for simplicity. This wave function which depends on a column vector with six entries,

$$\mathbf{C}(t) = (C_{12}, C_{13}, C_{14}, C_{23}, C_{24}, C_{34})^{\mathrm{T}}, \tag{8}$$

is a solution of the Schrödinger equation (5), for which the effective Hamiltonian is given as,

$$\mathbf{H}(t) = \begin{bmatrix} 0 & \Omega_{23}^* & 0 & 0 & 0 & 0 \\ \Omega_{23} & 0 & \Omega_{34}^* & \Omega_{12}^* & 0 & 0 \\ 0 & \Omega_{34} & 0 & 0 & \bar{\Omega}_{12}^* & 0 \\ 0 & \Omega_{12} & 0 & 0 & \bar{\Omega}_{34}^* & 0 \\ 0 & 0 & \bar{\Omega}_{12} & \bar{\Omega}_{34} & 0 & \bar{\Omega}_{23}^* \\ 0 & 0 & 0 & 0 & \bar{\Omega}_{23} & 0 \end{bmatrix}. \tag{9}$$

Here the time dependence of the Rabi frequencies $\Omega_{ij}(t) = |\Omega_{ij}(t)|\, e^{i\phi_{ij}}$ has been suppressed.

The analysis can be simplified if the Rabi frequencies satisfy the condition $\Omega_{ij}(t) = \bar{\Omega}_{ij}(t)$. In that case, the six adiabatic eigenvalues of the Hamiltonian $\mathbf{H}(t)$ are

$$\begin{aligned} \lambda_{1,2} &= 0, \\ \lambda_{3,4} &= \pm[(|\Omega_{12}| - |\Omega_{34}|)^2 + |\Omega_{23}|^2]^{1/2}, \\ \lambda_{5,6} &= \pm[(|\Omega_{12}| + |\Omega_{34}|)^2 + |\Omega_{23}|^2]^{1/2}. \end{aligned} \tag{10}$$

Since the eigenvalue $\lambda = 0$ is doubly degenerate, the Hilbert subspace of dark states is spanned by *two* linearly independent vectors

$$\begin{aligned} |A\rangle &= \Omega_{12}^*|12\rangle - \Omega_{23}|23\rangle + \Omega_{34}\, e^{2i\phi_{23}}|34\rangle, \\ |B\rangle &= \Omega_{34}^*|12\rangle - \Omega_{23}|14\rangle + \Omega_{12}\, e^{2i\phi_{23}}|34\rangle. \end{aligned} \tag{11}$$

In the absence of the third pulse $\Omega_{23}(t)$, the dark space is spanned by states $|12\rangle$ and $|34\rangle$. We will show that, when this pulse is switched on, the initially populated state $|12\rangle$ evolves, and ends in *one* of the states $|23\rangle$ ($|A\rangle$) or $|14\rangle$ ($|B\rangle$). This *bifurcation process* is controlled by the presence of nonadiabatic coupling, which always effects the dark states due to their degeneracy. In addition, the evolution is adiabatic if the time dependence of the relative change of the pulse envelopes is slow compared to the Rabi periods $1/\Omega_{ij}$ and $1/(|\Omega_{12}| - |\Omega_{34}|)$. The last criterion inevitably breaks down if the ratio $r = |\Omega_{12}/\Omega_{34}|$ approaches the value $r = 1$, where the system manifests an internal instability.

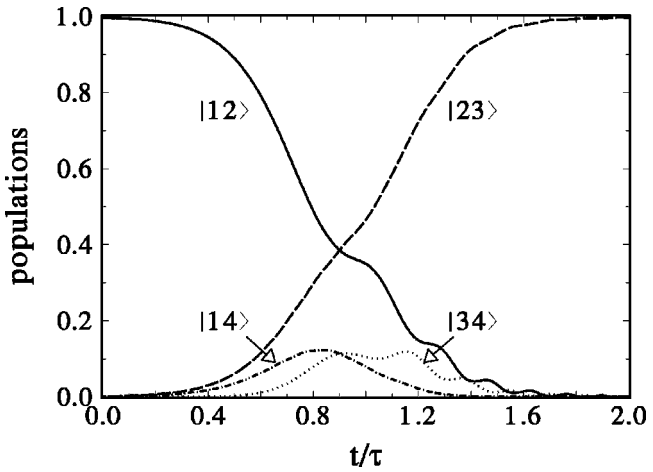

FIG. 3. Time-dependent populations of the two-electron states $|ij\rangle$. The population in state $|12\rangle$ is switched to state $|23\rangle$, while states $|14\rangle$ and $|34\rangle$ are populated only transiently.

B. Numerical results

In Fig. 3 we present the time-dependent populations $p_{ij} = |c_{ij}|^2$, calculated for Gaussian pulses $\Omega_{12}(t) = \Omega_{\max}\exp(-t^2/\tau^2)$, $\Omega_{34}(t) = \Omega_{12}(t)/r$, and $\Omega_{23}(t) = \Omega_{\max}\exp[-(t-t_0)^2/\tau^2]$. Here $\Omega_{\max}$ denotes the peak Rabi frequency, τ is the pulse length, and t_0 is the delay between the pulses. The settings $r = 1.25$, $t_0 = 2\tau$, and $\Omega_{\max} = 50/\tau$ of Fig. 3 cause the population in state $|12\rangle$ to switch to that of state $|23\rangle$ at the end of the process, with states $|14\rangle$ and $|34\rangle$ being populated only briefly. The small population oscillations shown in Fig. 3 reflect the effect of nonadiabaticity close to the critical value $r = 1$. The negligible populations of states $|13\rangle$ and $|24\rangle$ are not displayed.

In Fig. 4 we show final populations in the dark states as a

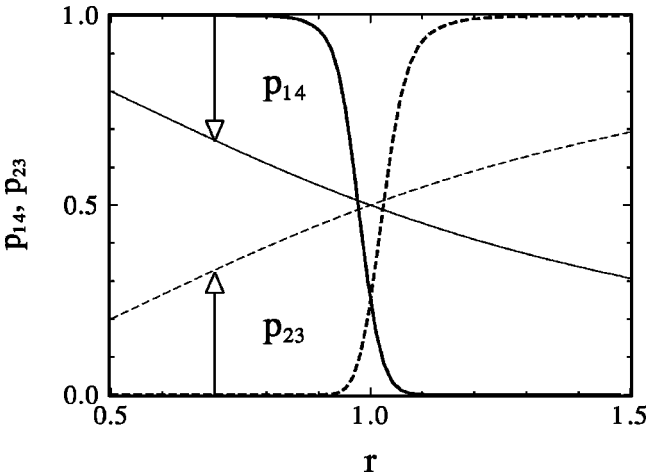

FIG. 4. Final populations of states $|14\rangle$ (solid line) and $|23\rangle$ (dashed line) as functions of the parameter r; other parameters are as in Fig. 3. The switching behavior around $r \approx 1$ changes to a splitting behavior (thin lines) in a reduced four-level system.

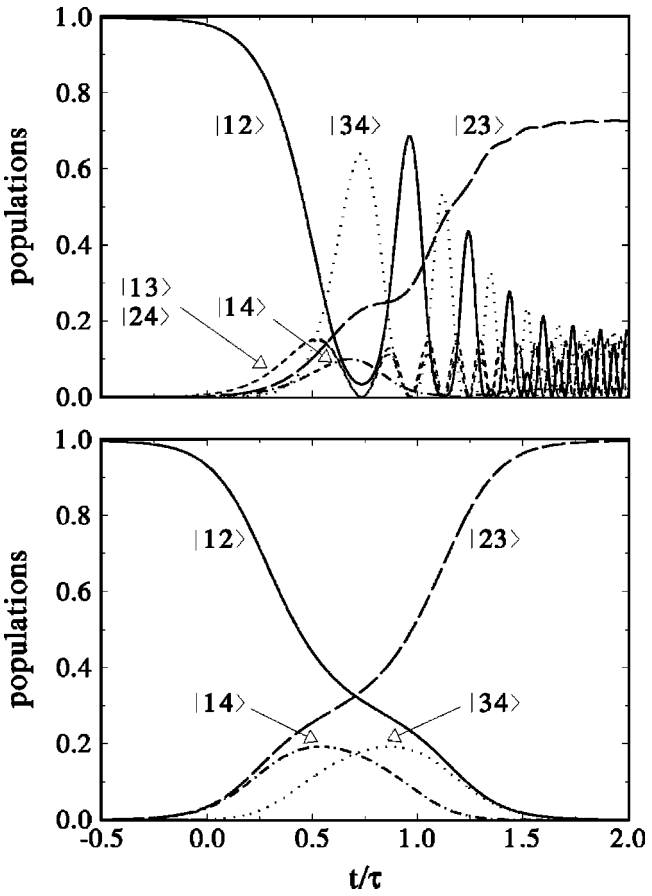

FIG. 5. Populations of the two-electron states $|ij\rangle$ in the (top) exact and (bottom) dark-state description. Parameters are as in Fig. 3, with $r=1.05$. We can see that the bifurcating behavior is preserved in the dark-state approximation.

function of r for the full six-level system (thick lines), and a reduced four-level system (thin lines), discussed below. The full system exhibits a bifurcating behavior leading to state $|14\rangle$ or $|23\rangle$, sharply dependent on the ratio r. If $r>1$, a hole STIRAP dominates, and the hole in level $|3\rangle$ is transported to level $|1\rangle$, thus populating state $|23\rangle$. If $r<1$, an electron STIRAP prevails; the electron initially in level $|2\rangle$ is transferred to level $|4\rangle$, and we end in state $|14\rangle$. The control over the final state takes place close to $r\approx 1$. The width of this region is determined by nonadiabatic coupling of the dark and nondark states. In this region, the system partly escapes from the dark subspace, and the sum of the final population in states $|14\rangle$ and $|23\rangle$ is lower than 1.

Our simulations show, that the bifurcation behavior displayed above is maintained even if the Rabi frequencies are different, $\Omega_{ij}(t)\neq\overline{\Omega}_{ij}(t)$, as long as they are of comparable magnitude. In this case, control over the choice between the final state $|14\rangle$ or $|23\rangle$ is achieved by altering the relative coupling strengths $|\Omega_{12}/\overline{\Omega}_{34}|$, $|\Omega_{34}/\overline{\Omega}_{12}|$. This competition can be represented by the ratio $R=|\Omega_{12}\overline{\Omega}_{12}/\Omega_{34}\overline{\Omega}_{34}|^{1/2}$, which in the degenerate case becomes $R=r$.

C. Discussion of the bifurcation behavior

To understand the bifurcation behavior, we transform the Schrödinger equation into the eigenstate basis [15]

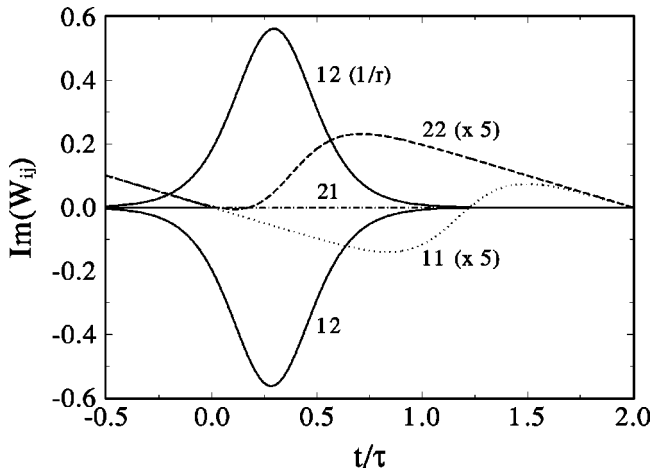

FIG. 6. Time-dependent behavior of the coefficients $\mathrm{Im}(W_{ij})$ $(i,j=1,2)$. The curves for $\mathrm{Im}(W_{ii})$ are magnified five times. The $\mathrm{Im}(W_{12})$ term dominates, and changes sign from negative to positive as $r\to 1/r$.

$$\dot{\mathbf{V}}(t)=-i\,\mathbf{W}(t)\,\mathbf{V}(t), \tag{12}$$

where the new state vector is $\mathbf{V}(t)=\mathbf{U}(t)\,\mathbf{C}(t)$. The matrix $\mathbf{U}(t)$ of eigenvectors diagonalizes Hamiltonian (9), and generates the coupling matrix

$$\mathbf{W}(t)\equiv\mathbf{U}^{-1}(t)\;\;\mathbf{H}(t)\;\;\mathbf{U}(t)+i\,\dot{\mathbf{U}}^{-1}(t)\;\;\mathbf{U}(t). \tag{13}$$

Using states $|A\rangle$ and $|B\rangle$ in Eq. (11), we can form new dark states $|A\rangle\pm r|B\rangle$, one of which is coupled to the initially populated $|12\rangle$ state. Then the matrix $\mathbf{U}(t)$, with columns of eigenvectors ordered as in Eq. (10), and the new dark states $|A\rangle\pm r|B\rangle$, has the analytic form

$$\mathbf{U}=\begin{bmatrix} 2\;\Omega_{12} & 0 & -\Omega_{23} & -\Omega_{23} & \Omega_{23} & \Omega_{23} \\ 0 & 0 & \mathcal{O}^- & -\mathcal{O}^- & -\mathcal{O}^+ & \mathcal{O}^+ \\ -\Omega_{23}r & \Omega_{23}r & \Delta\Omega^- & \Delta\Omega^- & \Delta\Omega^+ & \Delta\Omega^+ \\ -\Omega_{23} & -\Omega_{23} & -\Delta\Omega^- & -\Delta\Omega^- & \Delta\Omega^+ & \Delta\Omega^+ \\ 0 & 0 & -\mathcal{O}^- & \mathcal{O}^- & -\mathcal{O}^+ & \mathcal{O}^+ \\ \Omega_{34}f^+ & \Omega_{34}f^- & \Omega_{23} & \Omega_{23} & \Omega_{23} & \Omega_{23} \end{bmatrix}, \tag{14}$$

where

$$\mathcal{O}^\pm=\sqrt{(\Delta\Omega^\pm)^2+\Omega_{23}^2},\;\;\Delta\Omega^\pm=\Omega_{12}\pm\Omega_{34},$$

$$f^\pm=(1\pm r^2).$$

The coupling matrix $\mathbf{W}(t)$ can be obtained numerically from Eqs. (13) and (14).

To investigate the bifurcating control, we limit the solution of Eq. (12) to the two-dimensional dark subspace. This can be accomplished by decoupling eigenvectors 3–6 from the dark states by setting $W_{ij}(t)\equiv 0$ $(i,j>2)$. In Fig. 5 we show populations of the states $|ij\rangle$ in the exact (top) and dark-state (bottom) descriptions. The parameters are as in Fig. 3, but we use $r=1.05$, close to the critical value $r=1$. The exact solution oscillates due to nonadiabatic dynamics,

and only partly populates the final state $|23\rangle$. The dark-state solution is smooth, and *preserves* the bifurcating control in such a way, that fully populated final states $|12\rangle$ and $|23\rangle$ interchange exactly at $r=1$. If we only decouple eigenvectors 5 and 6 in Eq. (12), which have reasonably large eigenvalues even close to $r=1$, then the system basically follows the exact solution of Fig. 5 (top).

The reasons for the extensive control over the bifurcation process lies in the structure of this *e-h* symmetric system with six levels. The structure determines the coefficients W_{ij}, coupling the two dark states, shown in Fig. 6. The W_{12} term *dominates* and *changes sign* as $r=1.05\rightarrow 1/r$, and in this way affects which final state is populated. We can reduce the system to a four-level model (studied in Refs. [15,16]), by decoupling levels $|34\rangle$ and $|24\rangle$ in Fig. 2(b); decoupling just state $|34\rangle$ gives a five-level system with one dark state [16]. In the four-level case, with two dark states, the solution gives *split* populations $p_{14}=1/(1+r^2)$ and $p_{23}=r^2/(1+r^2)$, shown by thin lines in Fig. 4. In this simplified situation, the W_{12} term neither has such a dominant behavior nor does it change sign. It is even possible to find a dark-state vector $|D\rangle=(|\Omega_{12}|^2+|\Omega_{34}|^2)|12\rangle-\Omega_{12}\ \Omega_{23}|23\rangle-\Omega_{34}\ \Omega_{23}|14\rangle$ followed by this four-level system in the two-dimensional dark space, which does *not* show any sharp bifurcation behavior.

V. CONCLUSION

We have discussed the electron-hole symmetry in STIRAP's, leading to separate electron and hole excitation regimes. The regimes could realize transfers of electrons (holes) to high- (low-) energy orbitals. In a practical example, we have shown that a hole can be efficiently transferred into deep orbitals of a N_2 molecule. We have demonstrated that competition between electron and hole STIRAP's can lead to a new way of controlling bifurcating processes in molecular systems. We have found that other models with competition of several STIRAP's also lead to bifurcating behaviors.

ACKNOWLEDGMENTS

M. S. and P. K. acknowledge support from the U.S.-Israel BSF, the Minerva Foundation, and the BMBF Strategic Cooperation Project, Germany. J. F. would like to acknowledge I. Sh. Averbukh for support. This work was also partially supported by the National Science Foundation through a grant to the Institute for Theoretical Atomic and Molecular Physics at the Harvard-Smithsonian Center for Astrophysics.

[1] D. Grischkowsky and M. M. T. Loy, Phys. Rev. A **12**, 1117 (1975); **12**, 2514 (1975).
[2] F. T. Hioe, Phys. Lett. A **99**, 150 (1983); U. Gaubatz, P. Rudecki, M. Becker, S. Schiemann, M. Külz, and K. Bergmann, Chem. Phys. Lett. **149**, 463 (1988).
[3] K. Bergmann, H. Theuer, and B. W. Shore, Rev. Mod. Phys. **70**, 1003 (1998), and references therein.
[4] P. Dittman, F. P. Pesl, J. Martin, G. W. Coulston, G. Z. He, and K. Bergmann, J. Chem. Phys. **97**, 9472 (1992).
[5] M. Weitz, B. C. Young, and S. Chu, Phys. Rev. A **50**, 2438 (1994); C. Kulin *et al.*, Phys. Rev. Lett. **78**, 4815 (1997).
[6] A. Vardi, D. G. Abrashkevich, E. Frishman, and M. Shapiro, J. Chem. Phys. **107**, 6166 (1997).
[7] R. Wynar, R. S. Freeland, D. J. Han, C. Ryu, and D. J. Heinzen, Science **287**, 1016 (2000).
[8] A. Aspect, E. Arimodo, R. Kaiser, N. Vansteenkiste, and C. Cohen-Tannoudji, Phys. Rev. Lett. **61**, 826 (1988).
[9] S. E. Harris, J. E. Field, and A. Imamoglu, Phys. Rev. Lett. **64**, 1107 (1990).
[10] A. Imamoglu, D. D. Awschalom, G. Burkard, D. P. DiVincenzo, D. Loss, M. Sherwin, and A. Small, Phys. Rev. Lett. **83**, 4204 (1999).
[11] R. Sussmann, R. Neuhauser, and H. J. Neusser, J. Chem. Phys. **100**, 4784 (1994).
[12] G. Herzberg, *Molecular Spectra and Molecular Structure: I. Spectra of Diatomic Molecules*, 2nd ed. (Van Nostrand, Princeton, 1950).
[13] A. Lofthus and P. H. Krupenie, J. Phys. Chem. Ref. Data **6**, 113 (1977).
[14] R. E. Francke *et al.*, J. Chem. Phys. **72**, 1476 (1980); H.-J. Werner, J. Kalcher, and E.-A. Reinsch, *ibid.* **81**, 2420 (1984); L. G. Piper, *ibid.* **99**, 3174 (1993).
[15] R. Unayan, M. Fleischhauer, B. W. Shore, and K. Bergmann, Opt. Commun. **155**, 144 (1998).
[16] M. N. Kobrak and S. A. Rice, Phys. Rev. A **57**, 2885 (1998).